Fluorescence Properties and Photophysics of the Sulfoindocyanine Cy3 Linked Covalently to DNA

ARTICLE *in* THE JOURNAL OF PHYSICAL CHEMISTRY B · OCTOBER 2007

Impact Factor: 3.3 · DOI: 10.1021/jp072912u · Source: PubMed

4 AUTHORS:

Matthew Sanborn
University of California, Davis
41 PUBLICATIONS **229** CITATIONS
SEE PROFILE

Brian Connolly
Videojet
1 PUBLICATION **120** CITATIONS
SEE PROFILE

Kaushik Gurunathan
SASTRA University
8 PUBLICATIONS **228** CITATIONS
SEE PROFILE

Marcia Levitus
Arizona State University
54 PUBLICATIONS **1,461** CITATIONS
SEE PROFILE

Fluorescence Properties and Photophysics of the Sulfoindocyanine Cy3 Linked Covalently to DNA

Matthew E. Sanborn,[§,‡] Brian K. Connolly,[§,‡] Kaushik Gurunathan,[§,‡] and Marcia Levitus*[,§,†,‡]

Department of Chemistry and Biochemistry, Department of Physics and The Biodesign Institute, Arizona State University, Tempe, Arizona 85287-5601

Received: April 13, 2007; In Final Form: June 20, 2007

The sulfoindocyanine Cy3 is one of the most commonly used fluorescent dyes in the investigation of the structure and dynamics of nucleic acids by means of fluorescence methods. In this work, we report the fluorescence and photophysical properties of Cy3 attached covalently to single-stranded and duplex DNA. Steady-state and time-resolved fluorescence techniques were used to determine fluorescence quantum yields, emission lifetimes, and fluorescence anisotropy decays. The existence of a transient photoisomer was investigated by means of transient absorption techniques. The fluorescence quantum yield of Cy3 is highest when attached to the 5′ terminus of single-stranded DNA (Cy3−5′ ssDNA), and decreases by a factor of 2.4 when the complementary strand is annealed to form duplex DNA (Cy3−5′ dsDNA). Substantial differences were also observed between the 5′-modified strands and strands modified through an internal amino-modified deoxy uridine. The fluorescence decay of Cy3 became multiexponential upon conjugation to DNA. The longest lifetime was observed for Cy3−5′ ssDNA, where about 50% of the decay is dominated by a 2.0-ns lifetime. This value is more than 10 times larger than the fluorescence lifetime of the free dye in solution. These observations are interpreted in terms of a model where the molecule undergoes a *trans*−*cis* isomerization reaction from the first excited state. We observed that the activation energy for photoisomerization depends strongly on the microenvironment in which the dye is located. The unusually high activation energy measured for Cy3−5′ ssDNA is an indication of dye−ssDNA interactions. In fact, the time-resolved fluorescence anisotropy decay of this sample is dominated by a 2.5-ns rotational correlation time, which evidences the lack of rotational freedom of the dye around the linker that separates it from the terminal 5′ phosphate. The remarkable variations in the photophysical properties of Cy3−DNA constructs demonstrate that caution should be used when Cy3 is used in studies employing DNA conjugates.

Introduction

Fluorescence techniques are important tools for investigating the structure and dynamics of nucleic acids. The range of applications has increased significantly in the past years due to recent advances in solid-state chemical synthesis and the ready availability of reagents for conjugating probes to defined nucleotide positions. A wide variety of fluorescent modifications can be found nowadays in the catalogues of most custom DNA suppliers. Most frequently, fluorophores are incorporated at the 5′ terminus at the time of synthesis, using a specialized phosphoramidite reagent.[1]

Fluorescence resonance energy transfer (FRET) is one of the few tools available for measuring nanometer-scale distances and is one of the most widely used fluorescence techniques for investigating structure and dynamics of biopolymers.[2] For instance, FRET has been used to study the three-dimensional structure of the hammerhead ribozyme in solution,[3] the kinking of DNA and RNA helices by bulged nucleotides,[4] the solution structure of four-way DNA junctions,[5,6] and the helical handedness, twist, and rise of different DNA conformations.[7] More recently, advances in single-molecule detection have allowed the study of processes that are difficult to synchronize, opening up new opportunities to probe the dynamics of these systems.[8,9]

FRET applications rely on the assumption that the fluorescence properties of the probes are independent of the properties of the environment, so that any variations in the measured fluorescence intensity can be interpreted exclusively in terms of the changes in the conformation of the biopolymer under study. However, the photophysical properties of most fluorescent probes depend on the physical and chemical properties of the surroundings, which can lead to artifacts if the environment where the probes are located changes significantly during the biological process of interest.

Environmental effects are also critical in other types of fluorescence applications, where solvent properties such as temperature and viscosity are modified in order to characterize the system. For instance, the dependence of fluorescence anisotropy on temperature and viscosity can be used to study the rotational dynamics of the molecule to which the fluorophore is attached, from which information about aggregation state, size, and shape can be inferred.[10,11] Fluorescence anisotropy is also routinely used to characterize the rotational freedom of the linkage between the fluorophore and the macromolecule. This is particularly important in FRET applications because the rotational freedom of the fluorophores determines the orientation factor, which if unknown, results in an uncertainty in the measured distances.[12,13] Furthermore, fluorescence polarization

* Author to whom correspondence should be addressed. E-mail: marcia.levitus@asu.edu.
§ Department of Chemistry and Biochemistry.
‡ The Biodesign Institute.
† Department of Physics.

10.1021/jp072912u CCC: $37.00
Published on Web 08/24/2007

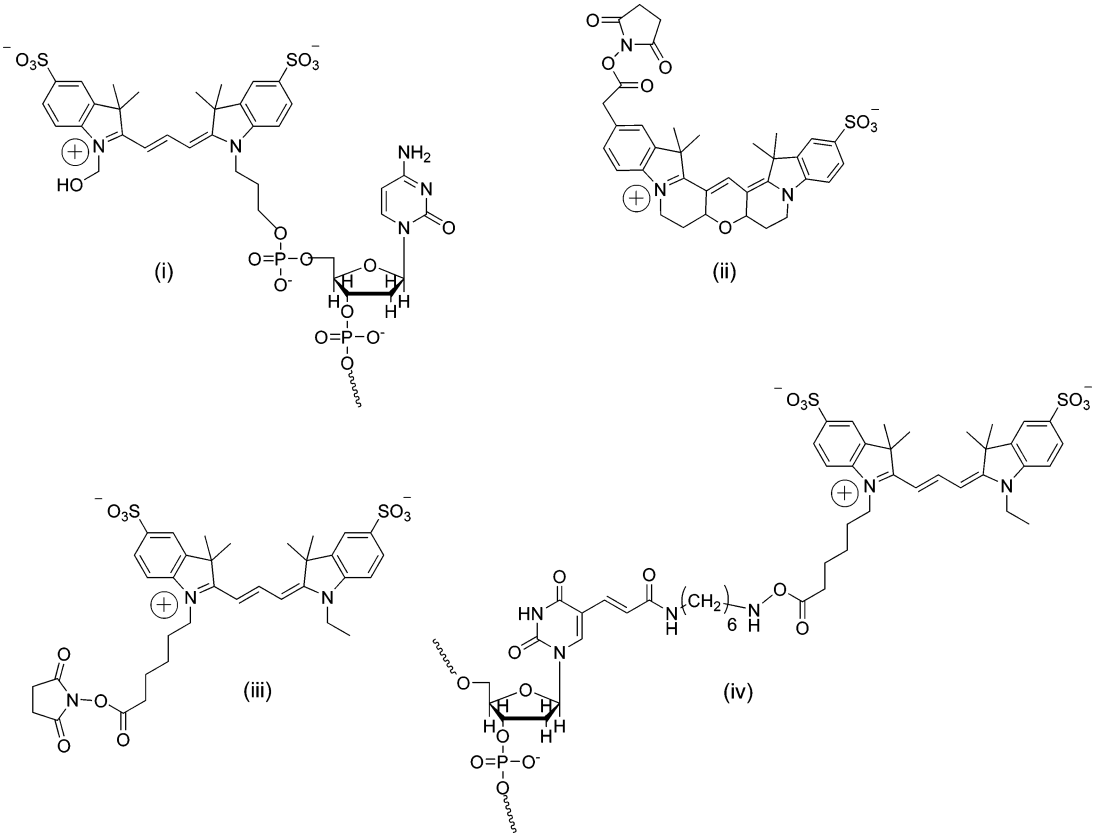

Figure 1. Structures of (i) Cy3−5′ DNA, (ii) free Cy3B, (iii) free Cy3, and (iv) Cy3-int DNA. The wavy lines in structures (i) and (iv) indicate binding to other nucleotides in the DNA chain.

has been used in single-molecule studies to characterize the kinetics of the rotation of molecular motors. In this case, a rigid linkage is desired so the polarization of the fluorescence emitted by the probe is a good reporter of the orientation of the protein to which the probe is attached.[14]

In this work, we investigate the photophysical properties of Cy3, a sulfoindocyanine widely used in fluorescence applications (Figure 1). Cy3 has been used in a large variety of studies, including the imaging of intracellular trafficking in living cells,[15−17] the study of protein−DNA and protein−protein interactions,[18−20] DNA structure,[7,11] etc. Moreover, Cy3 is one of the most popular fluorophores used in single-molecule applications, primarily due to its remarkable stability against photobleaching, compatibility with commonly available green lasers and avalanche photodiode detectors, and commercial availability.[8] Cy3 has been used in many single-molecule polarization studies of molecular motors[14] and in single-molecule FRET experiments in combination with the structurally related red-absorbing fluorophore Cy5.[8,21]

The photophysics of Cy5 has been investigated by several groups in the past decade, particularly in the context of elucidating the appearance of dark states in single-molecule fluorescence experiments.[22] The photoinduced isomerization and back-isomerization of Cy5 have been characterized by Widengren et al. using fluorescence correlation spectroscopy,[23] and more recently, Huang et al. characterized the spectroscopic behavior of this dye by means of ensemble and single-molecule measurements.[24]

However, despite its widespread popularity, the photophysics of Cy3 has not been investigated thoroughly to date. It has been well-established that carbocyanines with short polymethine chains (such as Cy3) photoisomerize from the first excited state more efficiently than the longer analogues (such as Cy5).[25] Thus, it is expected that Cy3 will be more sensitive than Cy5 to environmental factors such as temperature and local rigidity. This is particularly critical in FRET studies using Cy3 as the donor, since the efficiency of transfer is commonly calculated from the donor signal of samples containing both donor and acceptor, or only donor.[13] As we will show in this work, the fluorescence efficiency of Cy3 on DNA depends strongly on the specific location of the dye, complicating the determination of FRET efficiencies by this method.

There have been some scattered reports that document changes in the fluorescence properties of Cy3 upon covalent binding to biopolymers. Gruber et al. reported an anomalous fluorescence enhancement by 2−3 fold of Cy3 upon covalent linking to IgG and noncovalent binding to avidin.[26] More recently, Oiwa et al. measured the fluorescence lifetime and steady-state anisotropy of Cy3-labeled ATP and ADP analogues, and their complexes with myosin subfragment-1, observing an unexpected difference depending on whether the modification was at the 2′ or 3′ positions of the ribose moiety.[27] Also, in an attempt to characterize the interaction between Cy3 and duplex DNA, Norman et al. performed a combined NMR/fluorescence study which led to the conclusion that the fluorophore is stacked onto the end of the helix, in a manner similar to that of an additional base pair.[28] In this study, the authors interpret the high steady-state fluorescence anisotropies of the Cy3−DNA conjugates as evidence of restricted motion, but as we will prove in this work, the steady-state anisotropy of Cy3 is fairly insensitive to the environment, and is thus a bad indicator of rotational freedom.

Motivated by these observations, we investigated the photophysical behavior of the dye Cy3, both free in solution and covalently attached to DNA. Our results show that the photophysical properties of Cy3 can be explained in terms of a model

where the molecule undergoes a *trans*−*cis* isomerization reaction from the first excited singlet state. The activation energy for photoisomerization depends strongly on the rigidity of the microenvironment in which the dye is located. Since photoisomerization competes with fluorescence from the excited singlet state, the rigidity of the environment determines the fluorescence quantum yield and lifetime of the molecule. The existence of the photoisomer was confirmed by flash-photolysis and by comparison with the dye Cy3B, which has a rigid backbone that prevents isomerization (Figure 1). Unexpectedly, we observed that the highest isomerization barrier was for Cy3 attached to the 5′ terminus of single-stranded DNA. As a consequence, this sample showed the highest fluorescence efficiency and longest lifetime. Both values decrease upon annealing, indicating that the Cy3−DNA interactions in single-stranded DNA are disrupted upon duplex formation.

Materials and Methods

Materials. The following HPLC-purified DNA oligonucleotides and their complementary strands were obtained from Integrated DNA Technologies (Coralville, IA). Their purity was checked by 20% native polyacrylamide gel electrophoresis (PAGE).

Cy3-5' ssDNA: 5'-Cy3TTCTTCAGTTCAGCC-3'

Cy3-5' ssDNA2: 5'-Cy3CTCTTCAGTTCAGCC-3'

int ssDNA: 5'-GGCTGAAC/iAmMC6T/GAAGAG-3'

Here, 5′−Cy3 represents a Cy3 molecule attached covalently to the terminal 5′ phosphate of the DNA strand, and /iAmMC6T/ represents an internal amino-modified deoxy uridine (see Figure 1). Since no differences between the two 5′-labeled single-stranded sequences were observed, we will call them indistinctly Cy3−5′ ssDNA in the remainder of the manuscript.

The following nine oligonucleotides, with increasing number of nucleotides (n) ranging from 10 to 18, were additionally purchased. These strands are complementary to Cy3−5′ ssDNA and were used to generate duplex DNA with overhangs of various lengths.

5'GGCTGAACTGAAGAAGGT-3' (n = 18)
5'GGCTGAACTGAAGAAGG-3' (n = 17)
:
:
5'GGCTGAACTG-3' (n = 10)

Internally labeled Cy3−DNA (Cy3-int ssDNA) was prepared by reaction of int ssDNA with the monoreactive *N*-hydroxysuccinimidyl (NHS) ester of Cy3, following the recommendations of the supplier (GE Healthcare, Piscataway, NJ). The unreacted dye was removed by size exclusion chromatography using a 10DG column from Bio-Rad (Hercules, CA). The purity of the product was checked by gel electrophoresis.

Double-stranded DNA samples were prepared in 10 mM Tris buffer by mixing the Cy3-labeled strand with a 10% excess of the complementary strand to ensure absence of single-stranded, fluorescently labeled DNA. Native PAGE was used to verify proper annealing.

Solutions of the free dyes were prepared by dissolving the Cy3 or Cy3B monoreactive NHS esters in 10 mM Tris buffer.

Steady-State Fluorescence. Fluorescence spectra, fluorescence quantum yields (ϕ_f), and steady-state fluorescence anisotropies ($\langle r \rangle$) were measured on a QM-4/2005SE spectrofluorometer (PTI, NJ). Temperature was controlled using a water circulation system and was measured inside the cuvette with a calibrated thermocouple.

Fluorescence quantum yields were obtained at 22 °C using 5-carboxytetramethylrhodamine (TAMRA, Invitrogen, Carlsbad CA) in methanol as a reference ($\phi_f = 0.68$).[29] The absorbance of the sample and reference were kept below 0.05, and the difference in index of refraction between sample and reference was taken into account whenever necessary (e.g., measurements in glycerol). Fluorescence spectra were measured using polarizers in both the excitation and emission paths. The total fluorescence intensity was calculated as $I_T = I_{VV} + 2I_{VH}G$, where I is the fluorescence intensity, and the first and second subscript refer to the position of the excitation and emission polarizers respectively. The vertical orientation (V) denotes the direction perpendicular to the plane of the excitation and emission beams, and the horizontal orientation (H) is perpendicular to both V and to the direction of the propagation of the beam. The factor G accounts for the different sensitivities of the detection system for vertically and horizontally polarized light and is given by $G = I_{HV}/I_{HH}$. This experimental arrangement allows the simultaneous measurement of the total intensity and the steady-state fluorescence anisotropy. Furthermore, it eliminates the polarization artifacts encountered in measurements without polarizers of samples having large anisotropy values.[13]

Fluorescence quantum yields were calculated as a function of temperature in the 5−65 °C range using the value obtained at 22 °C as a reference. Corrections due to thermal expansion and changes in index of refraction with temperature were considered but turned out to be negligible in the studied temperature range.

The steady-state fluorescence anisotropy was calculated as $\langle r \rangle = (I_{VV} - GI_{VH})/I_T$ at different combinations of excitation and emission wavelengths in the main absorption band. The error of all steady-state measurements was estimated from the reproducibility of a series of identical measurements and was about 5% in most cases.

Time-Correlated Single-Photon Counting (TCSPC). Time-resolved fluorescence intensity and anisotropy measurements were performed using the time-correlated single-photon counting (TCSPC) technique. The excitation source was a Spectra-Physics (Tsunami) titanium sapphire (Ti:S) laser with 130-fs pulse duration operated at 80 MHz. Its fundamental output was sent through a frequency doubler and pulse selector (Spectra Physics, model 3980) to obtain 460-nm pulses at 4 MHz. The excitation beam was attenuated as needed to avoid pile-up effects. The sample was excited with vertically polarized light, and the fluorescence decay was collected with the emission polarizer kept at the magic angle with respect to the excitation polarizer. Fluorescence emission was collected at a 90° angle and detected using a double-grating monochromator (Jobin-Yvon, Gemini-180) and a microchannel plate photomultiplier tube (Hamamatsu R3809U-50). Data acquisition was performed using a single-photon counting card (Becker-Hickl, SPC-830). The instrument response function (IRF) was measured using a scattering solution (Ludox colloidal silica, Sigma). The measured fwhm was typically about 50 ps. The experimentally measured fluorescence decay, $F(t)$, is the convolution of the instrument response function with the intensity decay function, $I(t)$. Intensity decays were obtained from the measured decays by iterative deconvolution assuming that $I(t)$ can be represented by a sum of exponentials. The goodness of the fit was judged by the χ^2 value and the randomness of the residuals.

For anisotropy measurements, the fluorescence intensity decays were measured with the emission polarizer set at parallel

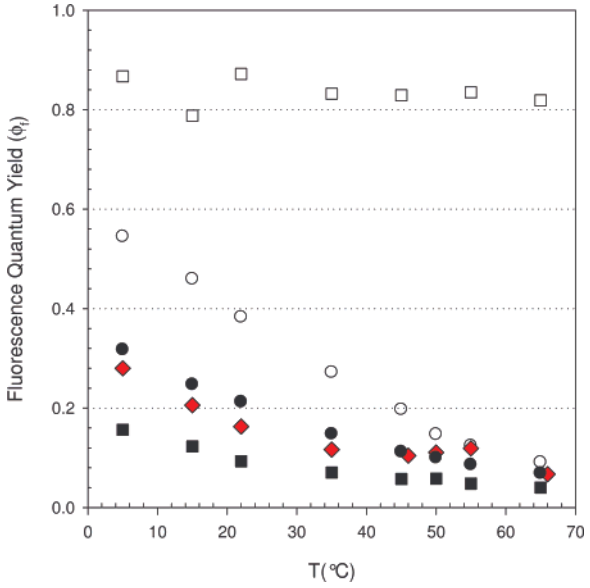

Figure 2. Fluorescence quantum yield of free Cy3 (■), Cy3B (□), and Cy3 on different DNA constructs: Cy3−5′ ssDNA (○), Cy3−5′ dsDNA (red ◆), and Cy3-int ssDNA (●). All measurements were performed in Tris buffer with 50 mM NaCl. The uncertainty in the determination is 10%. Values for Cy3-int dsDNA overlap with those for Cy3-int ssDNA, and are not shown for clarity.

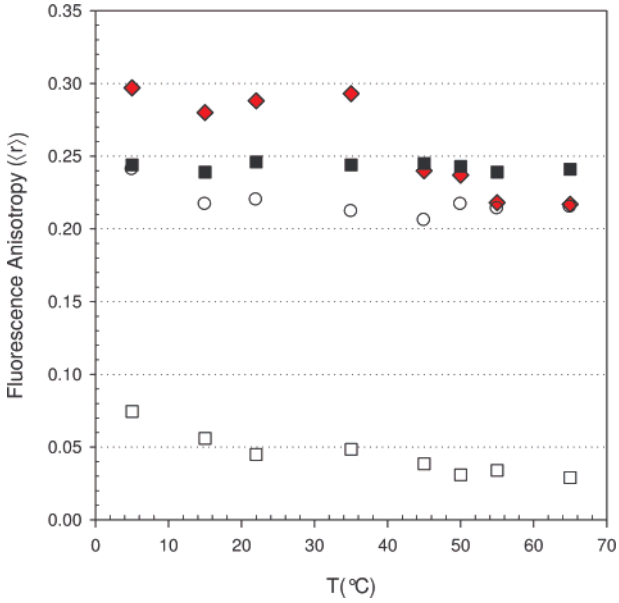

Figure 3. Steady-state fluorescence anisotropy ($\langle r \rangle$) of free Cy3 (■), Cy3B (□), and Cy3 on different DNA constructs: Cy3−5′ ssDNA (○) and Cy3−5′ dsDNA (red ◆). All measurements were performed in Tris buffer with 50 mM NaCl. Values for Cy3-int ssDNA and Cy3-int dsDNA overlap with those for free Cy3, and are not shown for clarity. Note that the abrupt decrease in $\langle r \rangle$ around 45 °C for Cy3−5′dsDNA is due to duplex melting.

or perpendicular orientation with respect to the excitation polarizer. The *G*-factor accounting for differences in system response for the two polarized emission components was determined by the tail matching method[30] using a solution of free Cy3B in water, for which the rotational correlation time (380 ps) is much faster than the fluorescence lifetime (2.7 ns). Time-resolved fluorescence anisotropy decays were calculated from the experimentally measured decays without deconvolution as $r(t) = (F_{VV} - F_{VH}\,G)/(F_{VV} + 2F_{VH}G)$. Since some of the decay times obtained by this procedure were just about 3 times the fwhm of our setup, we also calculated $r(t)$ by deconvolving F_{VV} and F_{VH} using arbitrary fitting functions, and creating $r(t)$ from the resulting functions.[30] This method yields time-dependent anisotropy curves free of convolution effects.

Flash Photolysis. Transient absorption was measured by flash photolysis using a Nd:YAG laser operating at 532 nm as the excitation source (pulse width ~5 ns). Details of this setup have been published elsewhere.[31] In essence, the monitoring beam was generated with a 150-W pulsed xenon arc lamp (Osram XBO 150/W) and passed through a monochromator. The two beams were focused through a small 1.5-mm aperture onto the sample, which was contained in a standard 1-cm path length cuvette. Light was detected using a photomultiplier tube, whose output was monitored with a digital oscilloscope.

Results

Fluorescence Quantum Yield and Steady-State Fluorescence Anisotropy of Free Cy3 And Cy3b. The steady-state fluorescence spectra, fluorescence quantum yields (ϕ_f), and steady-state fluorescence anisotropies ($\langle r \rangle$) of Cy3 and Cy3B were measured in Tris buffer as a function of temperature and ionic strength. All results were independent of the concentration of NaCl (0−1.5 M) and $MgCl_2$ (0−100 mM). The shape and peak position of the fluorescence emission spectrum of both dyes were independent of temperature in the studied range (5−65 °C).

For Cy3B, the efficiency of fluorescence showed practically no dependence on temperature (Figure 2, □). The measured fluorescence quantum yield was $\phi_f = 0.85$ at 22 °C, in agreement with the value provided by the supplier.[32] In contrast, Cy3 was significantly less fluorescent than Cy3B ($\phi_f = 0.09$ at 22 °C in Tris buffer), and showed a marked dependence on temperature (Figure 2, ■). Measured quantum yields decreased from $\phi_f = 0.16$ at 5 °C to $\phi_f = 0.04$ at 65 °C. In addition, ϕ_f for Cy3 was markedly dependent on viscosity. Measured values in pure glycerol were $\phi_f = 0.85$ independently of temperature in the 0−22 °C temperature range.

The steady-state fluorescence anisotropies of Cy3B in Tris buffer were low ($\langle r \rangle = 0.045$ at 22 °C) and decreased with increasing temperature as expected for a small molecule in aqueous solution (Figure 3). In contrast, values were fairly high for Cy3 ($\langle r \rangle = 0.246$ at 22 °C), and practically independent of temperature (Figure 3, ■). These results are consistent with the low fluorescence quantum yield and short lifetime of fluorescence of this dye and are similar to the anisotropy values reported for other short carbocyanines.[25,33] The maximum fluorescence anisotropy (r_0) was calculated as $r_0 = 0.386$ from measurements in glycerol between 0 and 20 °C. This value is very close to the maximum expected for an isotropic medium ($r_0 = 0.4$).

Fluorescence Quantum Yield and Steady-State Fluorescence Anisotropy of Cy3 on DNA. Covalent attachment to the 5′ terminus of single-stranded DNA had a small, but measurable effect on the position of the fluorescence emission spectrum of Cy3. A 4-nm shift to higher wavelengths was observed for Cy3−5′ ssDNA in Tris buffer, whereas no measurable differences were found for the other samples.

The fluorescence efficiency of Cy3 increased significantly upon covalent attachment to DNA in all cases. Values for Cy3−5′ ssDNA were the highest, and ranged from $\phi_f = 0.55$ at 5 °C to $\phi_f = 0.096$ at 65 °C, independently of whether the terminal 5′ nucleotide was a thymine or cytosine (Figure 2, ○). Surprisingly, these values decreased dramatically upon duplex formation at all temperatures (Figure 2, red ◆). The fluorescence efficiency of Cy3−5′ dsDNA increased around 45 °C and

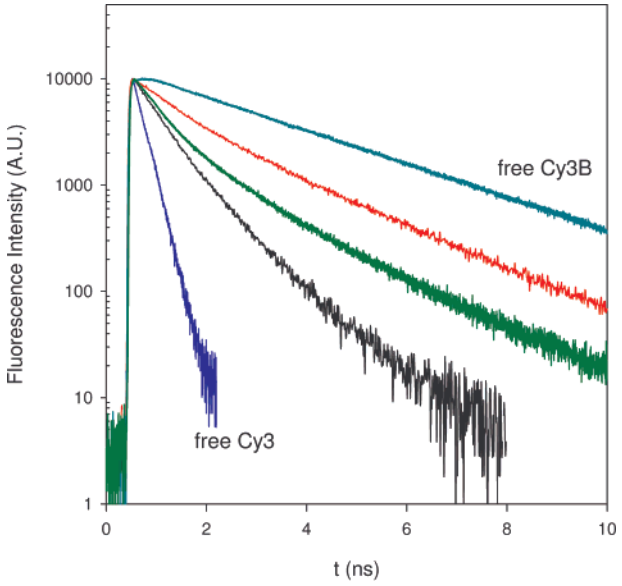

Figure 4. Time-resolved fluorescence decays measured by TCSPC. Free Cy3B (dark cyan), Cy3−5′ ssDNA (red), Cy3-int ssDNA (green), Cy3−5′ dsDNA (black), and free Cy3 (blue) Fluorescence lifetimes were obtained by deconvolution, assuming that the intensity decay can be represented by a sum of exponentials. The minimum number of exponential terms that produced randomly distributed residuals was used in this analysis. Fitting parameters are listed in Table 1.

matched the values determined for Cy3−5′ ssDNA above 50 °C, consistent with duplex melting.

The fluorescence efficiencies for single-stranded internally labeled DNA (Cy3-int ssDNA) were noticeably different from the corresponding values for the 5′-labeled sample (Figure 2, ●) and were not affected by duplex formation (values not shown for clarity).

Interestingly, covalent attachment to the 5′ terminus of ssDNA produced a decrease in the steady-state fluorescence anisotropy of Cy3 (Figure 3). The anisotropy values for Cy3−5′ ssDNA showed a small change at low temperatures, and remained constant at $\langle r \rangle \approx 0.21$ in the 15−65 °C range. Duplex formation at temperatures lower than the melting temperature increased the measured anisotropy to $\langle r \rangle \approx 0.29$. The measured anisotropies for both single-stranded and duplex internally labeled DNA (Cy3-int ssDNA and Cy3-int dsDNA) overlap within experimental error with those for the free dye in the whole temperature range, and are not shown for clarity.

All measured anisotropies and quantum yields were independent of NaCl (0−1.5 M) and $MgCl_2$ (0−100 mM) concentration.

Fluorescence Lifetimes. Fluorescence lifetimes were measured by pump−probe and time-correlated single-photon counting (TCSPC) at room temperature. Our pump−probe setup uses a 150-fs excitation pulse and an optical delay line which can control the time delay between the excitation and the probe pulses up to 3 ns. Longer lifetimes (up to 16 ns) were measured by TCSPC, which uses a ∼50-ps excitation pulse and therefore provides poorer time resolution in the subnanosecond time scale.

Free Cy3 and Cy3B. The TCSPC decays of the free dyes in Tris buffer were monoexponential. The measured lifetimes were 180 ± 10 ps for Cy3 and 2.70 ± 0.01 ns for Cy3B (Figure 4). Although the value measured for Cy3 is very close to the temporal instrumental response of our setup, it is identical within error to the result obtained from pump−probe experiments (see Supporting Information for representative pump−probe results).

Cy3−DNA Conjugates. Fluorescence lifetimes were measured in the same conditions described above. TCSPC and pump−probe results were consistent within error (see Supporting Information for representative pump probe results). Figure 4 shows the fluorescence decays obtained for Cy3−5′ ssDNA, Cy3−5′ dsDNA, and Cy3-int ssDNA by TCSPC. The decay for Cy3-int dsDNA overlaps with the corresponding decay for the corresponding single-stranded sample and is not shown for clarity.

Fluorescence decays for the DNA conjugates were fitted to the minimum number of exponential terms that produced randomly distributed residuals. The obtained lifetimes and relative amplitudes are listed in Table 1. The 5′-labeled ssDNA sample presented an unexpectedly long (2.0 ns) component that accounts for ∼50% of the decay (red curve, Figure 4). A similarly long component (1.9 ns) is also present in the internally labeled samples (green curve, Figure 4), although the relative weight is smaller in this case (∼14%). The two other lifetimes measured for Cy3-int ssDNA are in very good agreement with values previously published for a similar sample.[34]

Interestingly, the fluorescence decay of Cy3−5′ ssDNA becomes significantly faster upon duplex formation (black curve, Figure 4), which is consistent with the observed decrease in fluorescence quantum yield described above.

Time-Resolved Fluorescence Anisotropies. Time-resolved fluorescence anisotropies were measured by TCSPC and pump−probe as described in the experimental section. All experiments were performed in Tris buffer at 23 °C. The anisotropy decays of both free Cy3 and Cy3B measured by TCSPC were fitted to a monoexponential decay with a rotational correlation time of 380 ± 10 ps and an amplitude $r_0 = 0.38 \pm 0.01$ (Figure 5). The corresponding anisotropy decays obtained by pump−probe yield the same results within experimental error (see Supporting Information).

All anisotropy decays for the Cy3−DNA conjugates show a "fast" (<200 ps) and "slow" (>2.5 ns) component (Figure 5). The poor signal-to-noise ratio precludes attempts to analyze the

TABLE 1: Photophysical Properties of Cy3 and Cy3B[a]

	free Cy3B	free Cy3	Cy3−5′ ssDNA	Cy3−5′ ds DNA	Cy3-int ss DNA
ϕ_f (22 °C)	0.85 ± 0.01	0.09 ± 0.01	0.39 ± 0.01	0.16 ± 0.01	0.21 ± 0.01
$\langle r \rangle$ (22 °C)	0.045 ± 0.005	0.25 ± 0.01	0.22 ± 0.01	0.29 ± 0.01	0.24 ± 0.01
τ (ns)	2.7	0.18	2.0 (49%)	0.82 (44%)	1.9 (14%)
			0.53 (51%)	0.29 (56%)	0.76 (39%)
					0.24 (47%)
τ_r (ns)	0.38	0.38	2.5 (88%)	3.9 (82%)	2.7 (76%)
			0.18 (12%)	0.18 (18%)	0.17 (24%)
E_{Nt} (kJ/mol)		19 ± 1	33 ± 1	27 ± 1	25.2 ± 0.3

[a] The error of all steady-state measurements was estimated from the reproducibility of a series of identical measurements. Fluorescence lifetimes (τ) and rotational correlation times (τ_r) were obtained by fitting the decays of Figures 4 and 5 to the minimum number of exponential terms that produced randomly distributed residuals. Relative weights are quoted in parentheses. Activation energies (E_{Nt}) were obtained from Figure 8 according to eq 4.

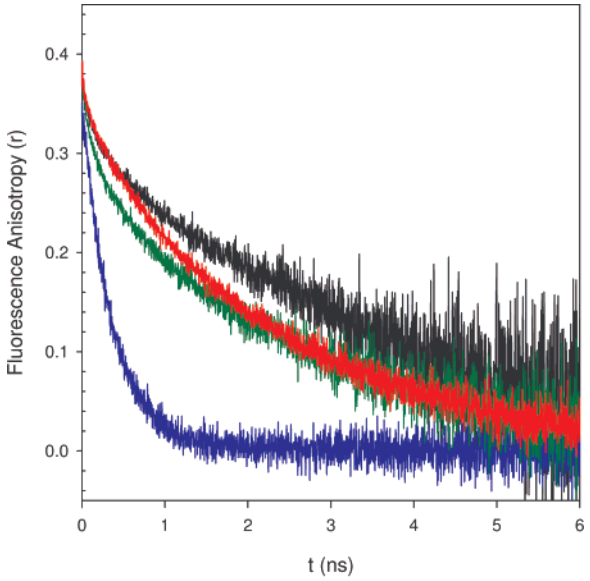

Figure 5. Time-resolved fluorescence anisotropy measured by TCSPC without deconvolution. Cy3−5′ dsDNA (black), Cy3−5′ ssDNA (red), Cy3-int ssDNA (green), and free Cy3 (blue). The decay of Cy3B overlaps with the corresponding decay for Cy3 and is not shown for clarity. Fitting parameters are listed in Table 1.

existence of more than two components in the anisotropy decays. Fluorescence anisotropy decays were obtained as described in the experimental section and fitted to the equation

$$r(t) = r_{01}\exp(-t/\tau_{r1}) + (0.38 - r_{01})\exp(-t/\tau_{r2})$$

where τ_{r1} and τ_{r2} are the rotational correlation times. The initial anisotropy, $r(t = 0)$, was fixed as 0.38, which is the value obtained from the anisotropy decay of the free dye, and the steady-state value measured in glycerol at 0 °C. Obtained fitting parameters are listed in Table 1.

To verify that the short rotational correlation times obtained in this procedure were not artifacts due to the fact that no deconvolution was performed, we alternatively obtained $r(t)$ by deconvoluting F_{VV} and F_{VH} prior to the calculation (see Materials and Methods). In this procedure, the experimentally measured intensity decays were first deconvoluted using four exponential terms as arbitrary fitting functions, and $r(t)$ was then created from the resulting functions. The anisotropy decays obtained by this method overlap within error with the decays obtained from the measured intensities without deconvolution, indicating that the short correlation times are reliable. Furthermore, the existence of the short correlation times was verified by pump−probe, which uses a 150-fs pulse and thus does not require deconvolution (see Supporting Information).

Laser Flash Photolysis. In flash photolysis, a laser pulse is used to produce a sufficient concentration of transient species suitable for spectroscopic observation. Transient states are monitored by changes in absorbance of a monitoring beam passing through the sample. The inset in Figure 6 shows a flash-photolysis trace of free Cy3 using $\lambda = 550$ nm (maximum of Cy3 absorption) as the monitoring beam. The absorbance decreases after the laser pulse, and recovers as the system decays to the ground state. The fact that the absorbance did not fully recover even after 10 μs is an indication of the existence of a long-lived transient state generated upon absorption. This state has been identified as the *cis*-isomer of Cy3 (Figure 7) by Huang et al.[24] The sign of ΔA depends on the relative value of the extinction coefficients of the generated species at the monitoring wavelength. A negative ΔA indicates that the ground state (gs) absorbs light more efficiently than the generated transient states (ts) at that particular wavelength ($\epsilon_\lambda^{gs} > \epsilon_\lambda^{ts}$).

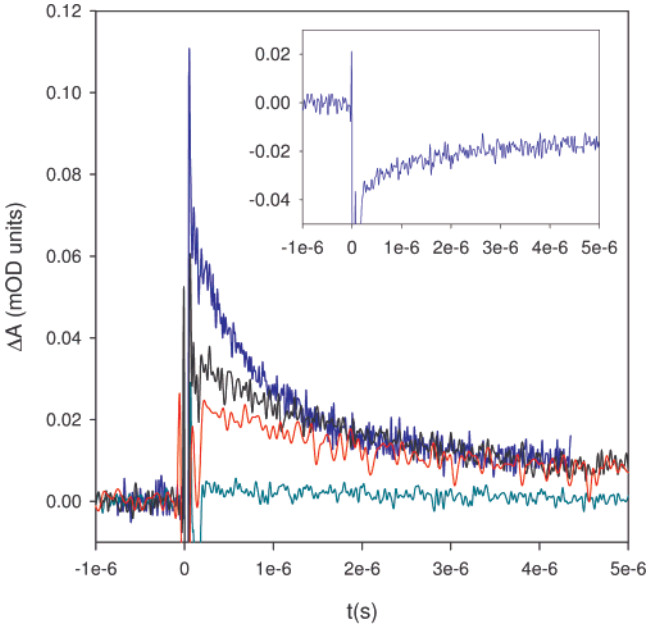

Figure 6. Flash-photolysis traces using a 570-nm probe beam. In order of decreasing amplitude: free Cy3 (highest amplitude, blue), Cy3−5′ dsDNA (black) Cy3−5′ ssDNA (red), and Cy3B (lowest amplitude, cyan). The absorbance of the dye at the excitation wavelength (532 nm) was matched in the different samples to allow a direct comparison of the amplitudes. Decays are multiexponential, and have a long-lived component in the ms-time scale (not shown). The signal decreases sharply initially due to fluorescence, limiting the time resolution to about 100 ns. (Inset) Free Cy3 probed at 550 nm.

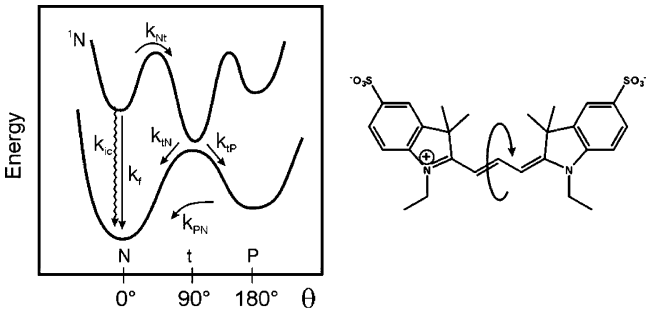

Figure 7. Potential energy surface for cyanine photoisomerization. θ represents the rotation coordinate, N the ground state of the normal form (*trans* isomer), ^{1}N the first excited singlet state of the normal form, t the twisted state, and P the ground state of the photoisomer.

A positive ΔA was observed at $\lambda = 570$ nm for all samples except Cy3B, which showed no measurable signal (Figure 6). The traces in Figure 6 were corrected for differences in sample absorbance, so the amplitudes are proportional to the quantum efficiency of formation of the transient state. A small ΔA does not necessarily indicate that the transient state is formed with small efficiency, but it might be a reflection of a small difference between the extinction coefficients ($\epsilon_\lambda^{gs} \approx \epsilon_\lambda^{ts}$).

Our results show an inverse correlation between the fluorescence quantum yield and the amplitude of the flash-photolysis signal (ΔA_0). This suggests that the transient state is generated from the first singlet excited state, and thus competes with fluorescence. The fact that Cy3B shows no measurable flash-photolysis signal at this wavelength is in agreement with the hypothesis that the transient state is generated by a conformational change in the Cy3 molecule that is repressed by the rigid backbone in Cy3B.

Flash-photolysis decays showed a complex multiexponential behavior with timescales spanning several orders of magnitude (μs−ms, not shown). In some cases, the ground state did not recover even after several milliseconds. The multiexponential behavior of the flash-photolysis decays can be interpreted in part by the fact that the triplet−triplet ($T_1 \rightarrow T_n$) absorption spectrum of Cy3 largely overlaps with the ground-state absorption of the *cis*-isomer (see Discussion).[35] Also, the existence of more than one isomer or a complex kinetic behavior of one individual isomer in the Cy3−DNA conjugates can contribute to the multiexponential behavior. A detailed kinetic analysis of the flash-photolysis decays of the Cy3−DNA conjugates is beyond the scope of this work and will be the subject of further investigations.

Discussion

The results obtained with free Cy3 are very similar to those reported for several related carbocyanines.[25,36,37] The photophysical properties of these dyes are usually interpreted in terms of the potential energy surface shown in Figure 7.[36,38] Following light absorption, the dyes isomerize from the first excited singlet state (^{1}N) to a ground-state photoisomer (P), which has been proposed to have a mono *cis* conformation. Isomerization occurs via a nonspectroscopic partially twisted intermediate excited state (t), which deactivates rapidly to the ground-state hypersurface to yield the ground-state photoisomer (P), or returns back to the thermodynamically stable ground state (N). Once formed, the photoisomer undergoes a thermal back-isomerization reaction to yield the thermodynamically stable isomer ($P \rightarrow N$).

The fluorescence quantum yield of Cy3 can be written in terms of the rate constants of the processes that occur from the first excited singlet state:

$$\phi_f(\text{Cy3}) = \frac{k_f}{(k_f + k_{ic} + k_{Nt}(T,\eta))} = k_f\tau \qquad (1)$$

Here, τ is the fluorescence lifetime, k_f refers to the radiative fluorescence rate, k_{ic} is the rate of internal conversion, and k_{Nt} is the rate of the twisting process that initiates isomerization. The efficiency of intersystem crossing has been measured as less than 0.3% for closely related carbocyanines; therefore, it will be disregarded in this analysis.[37] Isomerization is an activated process, and thus depends strongly on the temperature of the medium. Furthermore, since it involves a large molecular movement, it depends on the local microscopic viscosity (η). When the fluorescence decay is monoexponential, the fluorescence quantum yield and fluorescence lifetime are related through eq 1. Using the measured values of ϕ_f and τ for free Cy3 in Tris buffer at 22 °C, we calculate $k_f = 5 \times 10^8$ s^{-1}.

This photophysical model is consistent with the striking differences observed between Cy3 and Cy3B. In Cy3B, the rigid backbone prevents isomerization, so $k_{Nt} = 0$ in eq 1. As a consequence, the fluorescence quantum yield and lifetime of Cy3B are noticeably larger than the corresponding values for free Cy3, and no transient state can be detected by flash photolysis.

Cy3B as a Model Compound To Study Cy3 Isomerization. The viscosity of glycerol containing a few percent water increases by a factor of ~10 when decreasing the temperature from 20 to 0 °C.[39] This change in temperature and viscosity is expected to have a marked effect on ϕ_f (Cy3), unless $k_{Nt} \ll k_f$ (eq 1). The fact that we see no change in the efficiency of fluorescence of Cy3 in glycerol in the 0−22 °C range indicates that isomerization in these conditions is too slow to compete with fluorescence and internal conversion. Thus, in glycerol:

$$\phi_f(\text{Cy3,glycerol}) = k_f/(k_f + k_{ic}) \qquad (2)$$

Interestingly, we measured the same ϕ_f values for Cy3 in glycerol and Cy3B in Tris buffer. This suggests that the rigid backbone in Cy3B prevents isomerization without changing the Cy3 chromophore significantly; i.e. k_f and k_{ic} can be regarded as equal in Cy3 and Cy3B. Furthermore, the fact that the efficiency of fluorescence of Cy3B is fairly independent of temperature in the studied range suggests that the temperature dependence of k_{ic} can be ignored in this analysis.

From the above discussion it follows that

$$\phi_f^{-1}(\text{Cy3}) - \phi_f^{-1}(\text{Cy3B}) = \frac{k_{Nt}(T,\eta)}{k_f} \qquad (3)$$

writing k_{Nt} in terms of the Arrhenius equation, $k_{Nt} = A \exp(-E_{Nt}/RT)$:

$$\ln[\phi_f^{-1}(\text{Cy3}) - \phi_f^{-1}(\text{Cy3B})] = \ln(A/k_f) - E_{Nt}/RT \qquad (4)$$

Here, A is a constant that depends on the local microscopic friction, and E_{Nt} represents the activation energy for isomerization ($^1N \rightarrow t$), which includes both the electronic energy barrier and a friction-dependent term.[20] Strictly, k_{Nt} is not expected to have an Arrhenius behavior. The kinetics of barrier crossing in a viscous medium is usually described in terms of more complex models such as the Kramers equation, which have a viscosity-dependent pre-exponential factor. However, since the temperature dependence of viscosity can be described with an Arrhenius-like model, k_{Nt} can be satisfactorily fitted with an Arrhenius equation with a viscosity-dependent activation energy.[25]

Using the values measured in Tris buffer at 22 °C, ϕ_f (Cy3) = 0.09, τ (Cy3) = 180 ps, and ϕ_f (Cy3B) = 0.85, we obtain $k_{Nt} = 5 \times 10^9$ s^{-1} (eqs 1 and 3). This value is 1 order of magnitude higher than k_f, indicating that photoisomerization is a very efficient process for the free dye. Thus, isomerization is responsible for the low fluorescence quantum yield and short lifetime of free Cy3.

Figure 8 shows a plot according to eq 4. A constant value of ϕ_f (Cy3B) = 0.85 was used in this analysis. The activation energies for photoisomerization were calculated from these plots as 19 ± 1 kJ/mol (free Cy3), 25.2 ± 0.3 kJ/mol (Cy3-int ssDNA), 27 ± 1 kJ/mol (Cy3−5′ dsDNA), and 33 ± 1 kJ/mol (Cy3−5′ ssDNA). The value obtained for free Cy3 is very similar to the one reported for the closely related carbocyanine DiIC(2) in ethanol (E_{Nt} = 16.7 kJ/mol).[40] DiIC(2) (*N*,*N*′-diethyl-3,3′-tetramethylindocarbocyanine iodide) is identical to Cy3 except for the SO_3^- groups at the 5 and 5′ positions that are present in Cy3 to increase water solubility. Also, DiIC(2) lacks the modifications at the imine nitrogens, and thus isomerization is expected to happen with a lower activation barrier.

As expected, the lowest barrier for isomerization was measured for free Cy3. This is consistent with the results of the flash-photolysis experiments, which show a large-amplitude positive signal at 570 nm (Figure 6). Jia et al. performed a detailed analysis of the flash-photolysis decays of free Cy3 and concluded that about 65% of the transient absorption measured at 580 nm is due to ground-state absorption of the photoisomer.[35] The remaining 35% of the initial transient absorption was assigned to triplet−triplet absorption of the *trans*-isomer and accounts for the fast component of the flash-photolysis decay.

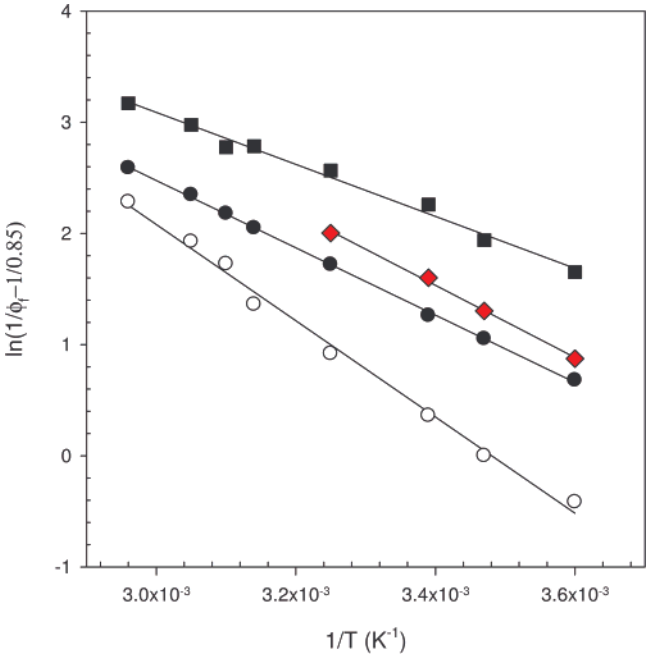

Figure 8. Plot according to eq 4. The activation energies for isomerization, calculated from the slopes of these plots, were: 19 ± 1 kJ/mol (free Cy3, ■), 25.2 ± 0.3 kJ/mol (Cy3-int ssDNA, ●), 27 ± 1 kJ/mol (Cy3−5′ dsDNA, red ◆), and 33 ± 1 kJ/mol (Cy3−5′ ssDNA, ○). The temperature range investigated for Cy3−5′ dsDNA is smaller due to duplex melting at higher temperatures.

Attachment of Cy3 to DNA increases the activation energy for isomerization (Figure 8, Table 1), and as a consequence, the amplitudes of the flash-photolysis decays decrease with respect to the value measured for the free dye. These observations are in agreement with the results of Åkesson et al., who observed a 3 kJ/mol increase in the isomerization barrier of DiIC in ethanol when increasing the length of the alkyl tail attached to the imine nitrogens from two (DiIC(2)) to 14 (DiIC(14))carbon atoms.[41] Thus, the attachment of a bulky substitutent such as a DNA strand is expected to produce a decrease in the isomerization rate, a concomitant increase in the fluorescence quantum yield and lifetime, and a decrease in the flash-photolysis amplitude. However, this alone does not explain the differences observed among the various DNA samples and, in particular, the surprisingly high activation energy measured for Cy3−5′ ssDNA. If the rate of isomerization were dictated by the size of the substitutent attached to Cy3, Cy3−5′ dsDNA would be expected to be more fluorescent than the corresponding single-stranded molecule. The fact that we see the opposite behavior suggests that the isomerization efficiency of Cy3 on DNA is also influenced by Cy3−DNA interactions.

Sabanayagam et al. reported TCSPC lifetime measurements of Cy3 conjugated to DNA using the same type of internal modification used here for Cy3-int dsDNA.[34] In this work, the authors interpret the non-monoexponential behavior of the decay as due to an equilibrium between two conformational states where the dye senses two environments of different polarity. However, the fluorescence efficiency of related carbocyanines has been shown to be dictated by the efficiency of isomerization that depends strongly on viscosity rather than polarity.[25] Thus, we favor a model where Cy3−DNA interactions increase the fluorescence efficiency of the dye as a result of an increase in the barrier for photoisomerization.

Cy3−DNA Interactions. Unexpectedly, Cy3 has the highest activation energy for isomerization when attached to the 5′ terminus of single-stranded DNA. In agreement with this observation, this sample presents the highest fluorescence quantum yield and smallest flash-photolysis amplitude of all studied Cy3 samples. The presence of a long-lived component in the fluorescence decay of this sample suggests that a fraction of the Cy3 molecules interact with the DNA strand so that the fluorophore experiences a high barrier for isomerization. The time-resolved fluorescence anisotropy decay of this sample provides another evidence of this interaction. The fast component in the anisotropy decay (180 ps) reflects the ability of the dye to depolarize emission by fast rotations around the three-carbon linker that separates the dye from the terminal DNA phosphate. However, 88% of the anisotropy decay is dictated by a 2.5-ns rotational correlation time, which indicates restricted mobility. A similar behavior was observed for a TAMRA−aptamer construct by Unruh et al.,[42] who measured a 5.0-ns component in the fluorescence anisotropy decay of this sample. In this work, the authors interpreted this result as evidence of TAMRA−aptamer interactions and suggested that the long rotational correlation time reflects the motion of the aptamer chain to which the dye is coupled. It is also interesting to compare the anisotropy decays of the two single-stranded samples. While the measured rotational correlation times are similar in both cases, the weight of the fastest component is largest for Cy3-int ssDNA, which has a six-carbon linker that provides more rotational freedom than the short linker that separates the Cy3 molecule from the terminal 5′ phosphate in Cy3−5′ ssDNA.

A possible model consistent with our results involves the existence of two populations, one in which Cy3 interacts strongly with the DNA strand and another one where the interaction is disrupted and isomerization occurs with a lower activation energy. Our results do not allow us to analyze the existence of more than two populations or whether these populations are in dynamic equilibrium in timescales longer than the fluorescence lifetime. The fact that the isomerization efficiency increases upon duplex formation indicates that the Cy3−ssDNA interaction is disrupted upon annealing. As a consequence, Cy3−5′ dsDNA is less fluorescent than Cy3−5′ ssDNA, its fluorescence quantum yield is more sensitive to temperature, and its fluorescence decay is faster. However, the 3.9-ns component that dominates the anisotropy decay of this sample suggests that the dye molecule is not entirely free to rotate around its linker. This long correlation time is consistent with the model proposed by Norman et al., who showed by NMR that Cy3 is stacked to the end of the double helix.[28] Yet, 18% of the anisotropy decay is dictated by a 180-ps rotational correlation time, and we found Cy3−5′ dsDNA to isomerize more efficiently than Cy3−5′ ssDNA. These photophysical observations suggest that Cy3−dsDNA interactions are dynamic in nature, in a way that allows a fraction of the fluorophores to isomerize and rotate around the linker fast enough to depolarize emission in the subnanosecond scale. Also, it should be noted that the results of the NMR studies represent the interactions between the ground state of Cy3 and the double helix, whereas the photophysical properties reported in this work reflect the interactions between the excited state of the dye and the DNA strand. It is possible that the dye−DNA stacking interactions observed in the NMR structure are disrupted in the excited state.

In order to gain a better understanding of the nature of the interactions between Cy3 and ssDNA, we measured the fluorescence quantum yield of Cy3−5′ ssDNA annealed to strands of various lengths (Figure 9). The fluorescence quantum yield remains close to the corresponding single-stranded value for $n = 10-13$, and shows a sharp decrease between $n = 13$

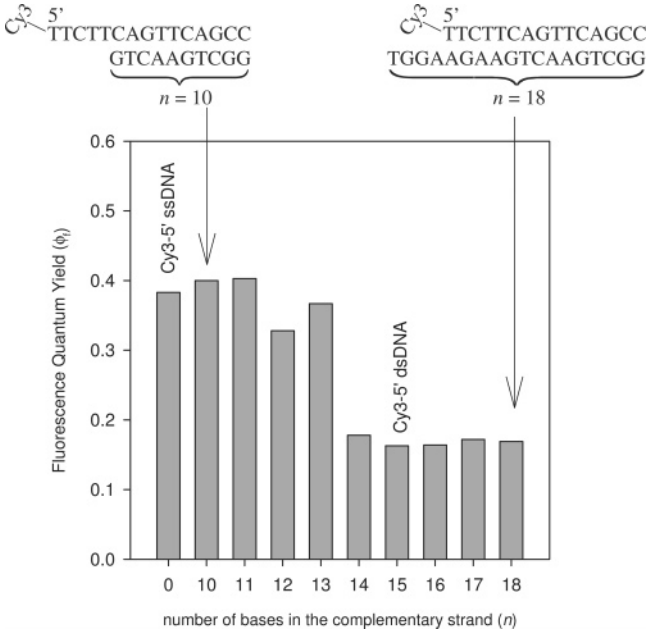

Figure 9. Fluorescence quantum yield of Cy3 on dsDNA with variable-length overhangs. The uncertainty in each determination is ~10%. $n = 15$ corresponds to Cy3−5′ dsDNA.

and $n = 14$ to the double-stranded value. No changes were observed when increasing the length of the complementary strand beyond $n = 15$. These results suggest that Cy3 bound to the 5′ terminus of single-stranded DNA interacts with the first two or three terminal bases. The fact that the activation energy for isomerization decreases upon annealing to the complementary strand suggests that this interaction is disrupted so that it probably involves an interaction between the dye and the nucleotide atoms involved in hydrogen bonding. These results are independent of whether the terminal nucleotide is a cytosine or a thymine, and more work is in progress to establish how DNA sequence plays a role in these interactions.

Several groups have reported nucleobase-specific quenching interactions of several fluorescent dyes.[43] Guanosine is the nucleoside with the lowest oxidation potential[44] and has been found to quench the excited states of rhodamines,[43] oxazines,[43] fuorescein,[45] and coumarin dyes[44] via photoinduced electron transfer. It is thus important to consider the possibility that photoinduced electron transfer affects the efficiency of fluorescence of Cy3 on DNA. Torimura et al. have measured the one-electron reduction potentials of several fluorescent dyes and found no peak above −1.0 V (vs NHE) for Cy3.[46] This indicates that quenching of Cy3 by any nucleoside is not thermodynamically favorable and should thus not be observed. This prediction was confirmed by standard Stern−Volmer experiments, where not only was no quenching observed, but the addition of deoxynucleosides to a solution of free Cy3 also produced an enhancement of the fluorescent signal.[46] Furthermore, the relative efficiency of fluorescence of Cy3 covalently bound to the 5′ terminus of DNA was shown to have a minimal (<10%) dependence on the nature of the adjacent nucleoside, including guanosine.[47] It has also been reported that other cyanines, such as Cy5, are not quenched by G-residues.[43]

Is $\langle r \rangle$ a Good Indicator of Cy3 Rotational Freedom? Steady-state anisotropy is very commonly used to evaluate the rotational freedom of a fluorophore. A high value is usually associated with a rotationally restricted environment and is often used as evidence of dye−DNA or dye−protein interactions.[11,28] For example, Norman et al.[28] measured steady-state anisotropies of duplex DNA containing a fluorescein and a Cy3 molecule at the 5′-termini. The high value reported for Cy3, $\langle r \rangle = 0.29$, was used in this work as evidence of constrained mobility and thus an indication of Cy3−DNA interactions. However, we argue that their interpretation of these high values as evidence of constrained mobility is not necessarily correct. As we proved for free Cy3, a short lifetime can give rise to an unusually high $\langle r \rangle$ value even in an unconstrained environment. In fact, our results show that the steady-state anisotropy of Cy3 is practically insensitive to the environment and does not provide direct information about rotational freedom. For example, the fact that the measured steady-state anisotropies for the free dye are actually higher than the values measured on Cy3−5′ ssDNA contradicts the common belief that attachment to a macromolecule increases the $\langle r \rangle$ value of the dye.

The steady-state anisotropy is the average of the anisotropy decay $r(t)$ over the intensity decay $I(t)$:[13]

$$\langle r \rangle = \frac{\int_0^\infty r(t)\, I(t)\, \mathrm{d}t}{\int_0^\infty I(t)\, \mathrm{d}t} \tag{5}$$

Rotational diffusion is expected to be the dominant mechanism of fluorescence depolarization. In the case of a prolate rotor, the anisotropy decay is a single exponential with a rotational correlation time (τ_r) that depends on temperature, viscosity, and the volume and shape of the molecule.

$$r(t) = r_0\, \mathrm{e}^{-t/\tau_r} \tag{6}$$

For a single-exponential intensity decay, eq 5 yields

$$\langle r \rangle = r_0(1 + \tau/\tau_r)^{-1} \tag{7}$$

Thus, $\langle r \rangle$ is not a direct measure of the rotational correlation time, but depends also strongly on the fluorescence lifetime. For example, the fluorescence lifetimes and rotational correlation times of free Cy3 and Cy3B listed in Table 1 can be used to calculate the expected steady-state anisotropies according to eq 7. Since the two molecules have basically the same shape and size, it is not surprising that the measured τ_r values are the same in both cases. Using $r_0 = 0.38$, and the τ_r and τ values obtained from time-resolved experiments (Table 1), we obtain $\langle r \rangle = 0.048$ for free Cy3B and $\langle r \rangle = 0.257$ for free Cy3. These values are in very good agreement with the measured steady-state anisotropies and exemplify the importance of considering the fluorescence lifetimes when analyzing steady-state anisotropy values.

The rotational correlation time is expected to be proportional to $1/T$, so $\langle r \rangle$ usually decreases with increasing temperature as was observed for Cy3B. However, since the first singlet excited state in Cy3 is depopulated also by photoisomerization, which is an activated process, the fluorescence lifetime decreases with increasing temperature as well. The overall temperature behavior of $\langle r \rangle$ depends on these competing factors. The fact that $\langle r \rangle$ is fairly constant for free Cy3 suggests that the rotational correlation time and fluorescence lifetime change at the same rate in the studied temperature range.

Time-resolved experiments show that the rotational correlation time increases significantly upon covalent binding to DNA, indicating a restricted motion. However, the same restriction causes an increase in the photoisomerization activation energy and a consequent increase in the fluorescence lifetime. As in the case of temperature, the overall effect of environmental restrictions on $\langle r \rangle$ is unpredictable. For example, for Cy3−5′ ssDNA, the increase in fluorescence lifetime overcomes the

increase in rotational correlational time, and as a consequence, $\langle r \rangle$ decreases with respect to the free dye. The increase in τ is not as marked for Cy3−5′ dsDNA (which has a lower isomerization barrier), yielding a larger $\langle r \rangle$ value. In conclusion, the complex dependence of the fluorescence lifetime of Cy3 with temperature and local friction makes the interpretation of the steady-state anisotropies difficult. Time-resolved experiments are required to investigate the rotational freedom of the dye in a direct manner.

Potential Sources of Artifacts in Energy-Transfer Experiments. FRET applications rely on the assumption that the fluorescence properties of the probes are independent of the properties of the environment, so that any variations in the measured fluorescence intensity can be interpreted exclusively in terms of the changes in the conformation of the biopolymer under study. However, we showed in this work that the fluorescence efficiency of Cy3 depends strongly on its local environment; thus, this assumption can lead to artifacts if the efficiency of transfer is not properly calculated and corrected.

These differences are most critical when Cy3 is used as a donor. The most common procedure to measure FRET efficiencies in a biochemistry laboratory involves measuring the donor steady-state intensity of the sample containing the FRET pair and comparing the result to the intensity of a reference containing only the donor. Our results show that this procedure can render inaccurate FRET efficiencies if the reference is not selected appropriately. A very simple illustration of this problem involves measuring the FRET efficiency of a Cy3−Cy5 double-labeled 15 bp-dsDNA that contains a fluorophore at each 5′ terminus. The correct FRET efficiency ($E = 0.5$) is obtained when Cy3−5′ dsDNA is used as a reference. However, if Cy3−5′ ssDNA is used instead, the calculated value would be $E = 0.78$. This striking difference is just a consequence of the difference in fluorescence quantum yield of Cy3 on single- or double-stranded DNA and exemplifies the importance of understanding the photophysical properties of Cy3. In contrast, in single-molecule experiments, FRET efficiencies are calculated from both the donor and acceptor intensities in the double-labeled sample. Yet, significant errors could be introduced if Cy3 is used to investigate dynamic processes involving DNA melting and annealing (such as the dynamics of DNA hairpins) or other processes where the local rigidity of the microenvironment sensed by Cy3 changes significantly. Changes in Cy3 intensity due to variations in the local environment can be erroneously interpreted as changes in FRET efficiency due to variations in donor−acceptor distance unless the photophysical properties of Cy3 are well characterized and understood.

Our results show that caution should be also used when calculating the Förster distance (R_0) of a FRET pair using Cy3 as the donor. This parameter, which measures the distance at which the FRET efficiency is 50%, depends on the fluorescence quantum yield of the donor ($R_0^6 \propto \phi_f$), which we proved to depend strongly on environmental factors. For instance, the fluorescence quantum yield of Cy3 on the 5′ terminus of ssDNA decreases by a factor of 2.4 when the DNA is annealed to its complementary strand, causing a decrease in R_0 by a factor of 1.15. This would represent a ∼7 Å change for a FRET pair with R_0 around 55 Å. Furthermore, R_0 depends on the so-called κ^2 factor, which takes into account the relative orientation of the donor and acceptor transition dipole moments. This factor has led to great discussion in the literature because it represents the major source of uncertainty in distance determinations by FRET.[12] If the donor and acceptor transition dipoles sample all orientations in a short time compared with the transfer time, the average orientation factor is $\kappa^2 = 2/3$. However, we have shown that the fluorescence anisotropy decays of Cy3 on DNA have a long-lived component that is longer than the corresponding fluorescence decays, and thus the assumption that Cy3 would sample all possible orientations is not appropriate. The structure proposed by Norman et al.[28] for Cy3−dsDNA suggests that one could calculate the κ^2 factor from the orientation of the molecule stacked on the double helix, assuming that Cy3 does not change orientations during its fluorescence lifetime. Yet, we showed that the anisotropy decay has a significant component that decays much faster than fluorescence; consequently, the assumption that the transition dipole of Cy3 does not rotate during transfer would not be suitable as well.

Conclusions

In conclusion, we showed that the photophysical properties of Cy3 on DNA depend strongly on its specific location and differ greatly from the properties of the free dye. This behavior is a consequence of the existence of a photoisomerization process that deactivates the first singlet excited state with an efficiency that depends strongly on the local microscopic friction. These differences complicate the interpretation of the steady-state anisotropies and FRET efficiencies and can introduce serious artifacts if the proper studies and controls are not carried out. Furthermore, we have shown that the steady-state anisotropy of Cy3 is fairly insensitive to the environment and is thus a bad indicator of rotational freedom. As a result, steady-state anisotropies of Cy3 should not be used to characterize the rotational mobility of Cy3 attached to biopolymers; time-resolved studies should be used instead.

Acknowledgment. We thank Su Lin and Ian Gould (ASU) for assistance with the time-resolved experiments, and Pedro Aramendía (University of Buenos Aires) for fruitful discussions.

Supporting Information Available: Representative fluorescence and anisotropy decays measured by pump−probe transient absorption spectroscopy. This material is available free of charge via the Internet at http://pubs.acs.org.

References and Notes

(1) Davies, M. J.; Shah, A.; Bruce, I. J. *Chem. Soc. Rev.* **2000**, *29*, 97.
(2) Selvin, P. R. *Nat. Struct. Biol.* **2000**, *7*, 730.
(3) Tuschl, T.; Gohlke, C.; Jovin, T. M.; Westhof, E.; Eckstein, F. *Science* **1994**, *266*, 785.
(4) Gohlke, C.; Murchie, A. I. H.; Lilley, D. M. J.; Clegg, R. M. *Proc. Natl. Acad. Sci. U.S.A.* **1994**, *91*, 11660.
(5) Eis, P. S.; Millar, D. P. *Biochemistry* **1993**, *32*, 13852.
(6) Clegg, R. M.; Murchie, A. I. H.; Lilley, D. M. J. *Biophys. J.* **1994**, *66*, 99.
(7) JaresErijman, E. A.; Jovin, T. M. *J. Mol. Biol.* **1996**, *257*, 597.
(8) Ha, T. *Methods* **2001**, *25*, 78.
(9) Tinnefeld, P.; Sauer, M. *Angew. Chem., Int. Ed.* **2005**, *44*, 2642.
(10) Jameson, D. M.; Sawyer, W. H. Fluorescence Anisotropy Applied to Biomolecular Interactions. In *Biochemical Spectroscopy*; Sauer, K., Ed.; Methods in Enzymology, Vol. 246; Academic Press: San Diego, 1995; pp 283.
(11) Fogg, J. M.; Kvaratskhelia, M.; White, M. F.; Lilley, D. M. J. *J. Mol. Biol.* **2001**, *313*, 751.
(12) Dale, R.; Eisinger, J.; Blumberg, W. *Biophys. J.* **1979**, *26*, 161.
(13) Valeur, B. *Molecular Fluorescence: Principles and Applications*; Wiley-VCH: Weinheim, Germany, 2001.
(14) Adachi, K.; Yasuda, R.; Noji, H.; Itoh, H.; Harada, Y.; Yoshida, M.; Kinosita, K. *Proc. Natl. Acad. Sci. U.S.A.* **2000**, *97*, 7243.
(15) Bastiaens, P. I. H.; Majoul, I. V.; Verveer, P. J.; Soling, H. D.; Jovin, T. M. *EMBO J.* **1996**, *15*, 4246.
(16) Bornfleth, H.; Edelmann, P.; Zink, D.; Cremer, T.; Cremer, C. *Biophys. J.* **1999**, *77*, 2871.
(17) Tani, T.; Miyamoto, Y.; Fujimori, K. E.; Taguchi, T.; Yanagida, T.; Sako, Y.; Harada, Y. *J. Neurosci.* **2005**, *25*, 2181.
(18) Martinez-Senac, M. M.; Webb, M. R. *Biochemistry* **2005**, *44*, 16967.

(19) Kozlov, A. G.; Lohman, T. M. *Biochemistry* **2002**, *41*, 6032.
(20) Kenworthy, A. K. *Methods* **2001**, *24*, 289.
(21) Murphy, M. C.; Rasnik, I.; Cheng, W.; Lohman, T. M.; Ha, T. J. *Biophys. J.* **2004**, *86*, 2530.
(22) Sabanayagam, C. R.; Eid, J. S.; Meller, A. *J. Chem. Phys.* **2005**, *123*, 224708.
(23) Widengren, J.; Schwille, P. *J. Phys. Chem. A* **2000**, *104*, 6416.
(24) Huang, Z. X.; Ji, D. M.; Wang, S. F.; Xia, A. D.; Koberling, F.; Patting, M.; Erdmann, R. *J. Phys. Chem. A* **2006**, *110*, 45.
(25) Aramendia, P. F.; Negri, R. M.; San Roman, E. *J. Phys. Chem.* **1994**, *98*, 3165.
(26) Gruber, H. J.; Hahn, C. D.; Kada, G.; Riener, C. K.; Harms, G. S.; Ahrer, W.; Dax, T. G.; Knaus, H. G. *Bioconjugate Chem.* **2000**, *11*, 696.
(27) Oiwa, K.; Jameson, D. M.; Croney, J. C.; Davis, C. T.; Eccleston, J. F.; Anson, M. *Biophys. J.* **2003**, *84*, 634.
(28) Norman, D. G.; Grainger, R. J.; Uhrin, D.; Lilley, D. M. J. *Biochemistry* **2000**, *39*, 6317.
(29) Magde, D.; Brannon, J. H.; Cremers, T. L.; Olmsted, J. *J. Phys. Chem.* **1979**, *83*, 696.
(30) O'Connor, D. V.; Phillips, D. *Time-Correlated Single Photon Counting*; Academic Press: London, 1984.
(31) Gould, I. R.; Ege, D.; Moser, J. E.; Farid, S. *J. Am. Chem. Soc.* **1990**, *112*, 4290.
(32) Cooper, M.; Ebner, A.; Briggs, M.; Burrows, M.; Gardner, N.; Richardson, R.; West, R. *J. Fluoresc.* **2004**, *14*, 145.
(33) Levitus, M.; Negri, R. M.; Aramendia, P. F. *J. Phys. Chem.* **1995**, *99*, 14231.
(34) Sabanayagam, C. R.; Eid, J. S.; Meller, A. *J. Chem. Phys.* **2005**, *122*.
(35) Jia, K.; Wan, Y.; Xia, A. D.; Li, S. Y.; Gong, F. B.; Yang, G. Q. *J. Phys. Chem. A* **2007**, *111*, 1593.
(36) Chibisov, A. K.; Zakharova, G. V.; Gorner, H.; Sogulyaev, Y. A.; Mushkalo, I. L.; Tolmachev, A. I. *J. Phys. Chem.* **1995**, *99*, 886.
(37) Chibisov, A. K.; Zakharova, G. V.; Gorner, H. *J. Chem. Soc., Faraday Trans.* **1996**, *92*, 4917.
(38) Velsko, S. P.; Waldeck, D. H.; Fleming, G. R. *J. Chem. Phys.* **1983**, *78*, 249.
(39) *CRC Handbook of Chemistry and Physics*, 87th ed.; CRC: Boca Raton, FL, 2006.
(40) Korppitommola, J. E. I.; Hakkarainen, A.; Hukka, T.; Subbi, J. *J. Phys. Chem.* **1991**, *95*, 8482.
(41) Akesson, E.; Hakkarainen, A.; Laitinen, E.; Helenius, V.; Gillbro, T.; Korppitommola, J.; Sundstrom, V. *J. Chem. Phys.* **1991**, *95*, 6508.
(42) Unruh, J. R.; Gokulrangan, G.; Lushington, G. H.; Johnson, C. K.; Wilson, G. S. *Biophys. J.* **2005**, *88*, 3455.
(43) Heinlein, T.; Knemeyer, J. P.; Piestert, O.; Sauer, M. *J. Phys. Chem. B* **2003**, *107*, 7957.
(44) Seidel, C. A. M.; Schulz, A.; Sauer, M. H. M. *J. Phys. Chem.* **1996**, *100*, 5541.
(45) Nazarenko, I.; Lowe, B.; Darfler, M.; Ikonomi, P.; Schuster, D.; Rashtchian, A. *Nucleic Acids Res.* **2002**, *30*, e37.
(46) Torimura, M.; Kurata, S.; Yamada, K.; Yokomaku, T.; Kamagata, Y.; Kanagawa, T.; Kurane, R. *Anal. Sci.* **2001**, *17*, 155.
(47) Behlke, M.; Huang, L.; Bogh, L.; Rose, S.; Devor, E. Fluorescence quenching by proximal G bases. http://www.idtdna.com/support/technical/TechnicalBulletinPDF/Fluorescence_quenching_by_proximal_G_bases.pdf (accessed June 2007)